An Artificial Neural Network Controller for Three-level Shunt Active Filter to Eliminate the Current Harmonics and Compensate Reactive Power

Chennai Salim[1], M.T Benchouia[2]
1- Department of Electrical Engineering, Nuclear Research Center of Birine, Algeria.
Email: chenaisalimov@yahoo.fr (Corresponding author)
2- Laboratory L.G.E.B., Department of Electrical Engineering, Biskra University, Algeria.
Email: benchouiat@yahoo.fr

Received: March 2011 Revised: May 2011 Accepted: July 2011

ABSTRACT:
The increased use of nonlinear devices in the industry has resulted in the direct increase of harmonic distortion in power systems during these last years. Active filter systems are proposed to mitigate current harmonics generated by nonlinear loads. The conventional scheme based on a two-level voltage source inverter controlled by a hysteresis controller has several disadvantages and cannot be used for medium or high-power applications. To overcome these drawbacks and improve the APF performance, there's a great tendency to use multilevel inverters controlled by intelligent controllers. Three level (NPC) inverter is one of the most widely used topologies in various industrial applications such as machine drives and power factor compensators. On the other hand, artificial neural networks are under study and investigation in other power electronics applications. In order to gain the advantages of the three-level inverter and artificial neural networks and to reduce the complexity of classical control schemes, a new active power filter configuration controlled by two MLPNN (Multi-Layer Perceptron Neural Network) is proposed in this paper. The first ANN is used to replace the PWM current controller, and the second one to maintain a constant dc link voltage across the capacitors and compensate the inverter power losses. The performance of the global system, including power and control circuits is evaluated by Matlab-Simulink and SimPowerSystem Toolbox simulation. The obtained results confirm the effectiveness of the proposed control scheme.

KEYWORDS: Artificial neural networks, MLPNN current controller, MLPNN voltage controller, Three-level shunt active filter, Synchronous current detection method, Current harmonics.

1. INTRODUCTION

A large part of total electrical energy, produced in the world, supplies different types of non-linear loads such as variable frequency drives and electronic ballasts, which does not resemble the grid sinusoidal voltage. This load is typically composed of odd order currents, which are expressed as multiples of the fundamental frequency. The harmonic current cannot contribute to active power and need to be eliminated to enhance the power quality [1]. Conventionally, passive filters have been used to eliminate current harmonics and to increase the power factor. However, the use of passive filter has many disadvantages. Active Power Filter (APF) is the popular solution used to eliminate the undesired current components by injection of compensation currents in opposition to them [2]. The common power converter used is the two-level voltage source inverter [3]-[4]. Due to power handling capabilities of power semiconductors, these inverters are limited for low power applications.

The performance of any shunt active filter (SAF) is based on three essentials design criteria: power inverter topology, control strategy and current controller. Today three-level inverter is one of the most multilevel topology widely employed and applied in medium and high-power applications [1]-[5]. The principally control techniques used to determining the reference currents are the instantaneous power theory [6] and the synchronous reference frame detection method [7], these techniques include a much number of calculation, complex mathematical transformation and are difficult to implement practically [8]. The synchronous current detection technique is another method widely used, it is easy to implement, required less computational efforts than power reactive theory (PQ) or synchronous reference frame (SRF) methods and gives excellent results.

The controller is an important element of the active

power filter operation and has been a subject of several researches in recent years [9]-[10] particularly the PWM technique controls proposed for high power or medium-voltage applications such as reactive power compensation and AC motor drives. However, these techniques present some drawbacks; to overcome their disadvantages and improve the APF performances, there's a great tendency to use intelligent techniques particularly neural network controllers. The first studies have shown that ANNs are reliable in improvement of power electronic systems control [11]-[12]. Some other research works were elaborated using ANNs based a two-level VSI in the last years, and they have given satisfactory results [13].

This paper presents a new control scheme for three-level neutral point clamped (NPC) shunt active filter based on two MLPNNs. The performances of proposed APF are evaluated through computer simulations for transient and steady-state conditions using Matlab-Simulink software and SimPowerSystem Toolbox.

The shunt active power filter compensation principle is shown in Figure 1. It is controlled to cancel current harmonics on AC side and makes the source current in phase with the voltage source. The current source after compensation becomes sinusoidal and in phase with the voltage source [14]-[15].

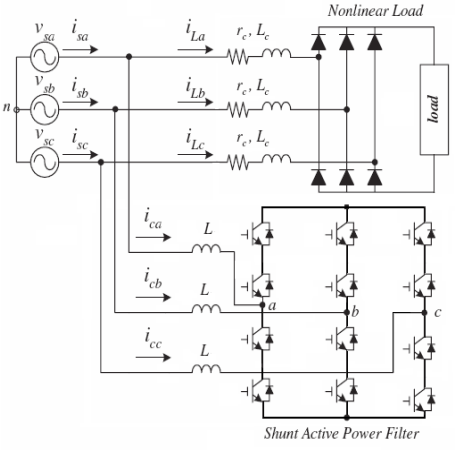

Fig. 1. Three-level shunt active filter

Multilevel inverters are being investigated and recently used for active filter topologies. Three-level inverter is becoming very popular today for most industrial applications, such as machine drives and power factor compensators. These advantages are reduction of the harmonic content generated by the active filter and decrease the voltage or current ratings of the semiconductors [16]. Figure 2 shows the circuit topology of a diode-clamped three-level inverter based on the six main switches (T_{11}, T_{21}, T_{31}, T_{14}, T_{24}, T_{34}) of the traditional two-level inverter, adding six auxiliary switches (T_{12}, T_{13}, T_{22}, T_{23}, T_{32}, T_{33}) and two neutral clamped diodes on each bridge arm respectively. The diodes are used to make the connection with the point of reference to obtain Midpoint voltages. Such structure allows the switches to endure larger dc voltage input on the premise of not raising the level of their withstand voltage. Moreover, take phase-A as example, three values of voltage level $U_{dc}/2$, 0 and $-U_{dc}/2$ can be output corresponding to three switching states A, 0, B. listed in Table (1). As a result, there exist 27 states of switching output from the three-phase three-level [17]-[18].

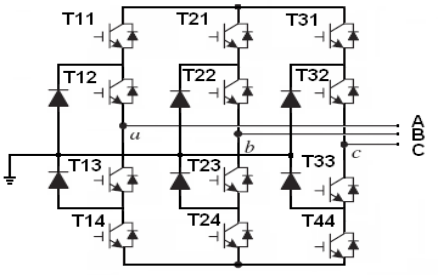

Fig. 2. Circuit topology of three-level NPC inverter

Table 1. Switching states of three-level inverter

Switching States	Voltage output	T11	T12	T13	T14
A	$U_{dc}/2$	ON	ON	OFF	OFF
0	0	OFF	ON	ON	OFF
B	$-U_{dc}/2$	OFF	OFF	ON	ON

2. CONTROL STRATEGY

2.1. Synchronous current detection method

The control strategy adopted in this work to estimate the reference signals required to compensate current harmonics is the synchronous current detection method. It's easy to implement and requires few number computations compared to others control method [19]-[20]. The compensating currents of active filter are calculated by sensing the load currents. The current delivered by a DC voltage regulator, I^*_{smd}, the AC voltage of source peak V_{sm} and the zero crossing point of source voltage. The expression of the AC source voltage at the point of common coupling is given by:

$$v_{sa}(t) = V_{sm} \cdot \sin(\omega t)$$
$$v_{sb}(t) = V_{sm} \cdot \sin(\omega t - \frac{2\pi}{3}) \quad (1)$$
$$v_{sc}(t) = V_{sm} \cdot \sin(\omega t - \frac{4\pi}{3})$$

In order to compensating the current harmonics, the average active power of AC source must be equal with average active power load (P_{Lav}), with considering the unity power factor of AC source side currents the average active power can be calculated as bellow:

$$P_s = \frac{3}{2} V_{sm} . I^*_{smp} = P_{Lav} \quad (2)$$

I*smp is the first component of AC side current.

From equation (2), I*smp can be calculated as bellow:

$$I^*_{smp} = \frac{2}{3} \frac{P_{Lav}}{V_{sm}} \quad (3)$$

The second component of AC source current I*smd is obtained from the DC capacitor voltage regulator. The desired peak current of AC source can be calculated as bellow:

$$I^*_{sm} = I^*_{smp} + I^*_{smd} \quad (4)$$

The AC source currents must be sinusoidal and in phase with source voltages, these currents can be calculated with multiplying the peak source current to a unity sinusoidal signal, that these unity signals can be obtained from equation (5):

$$i_{ua}(t) = v_{sa} / V_{sm}$$
$$i_{ub}(t) = v_{sb} / V_{sm} \quad (5)$$
$$i_{uc}(t) = v_{sc} / V_{sm}$$

The desired source side currents can be obtained from equation (6):

$$i^*_{sa}(t) = I^*_{sm} . i_{ua}$$
$$i^*_{sb}(t) = I^*_{sm} . i_{ub} \quad (6)$$
$$i^*_{sc}(t) = I^*_{sm} . i_{uc}$$

Finally, the reference currents of AF can be obtained from (7):

$$i^*_{ca} = i^*_{sa} - i_{La}$$
$$i^*_{cb} = i^*_{sb} - i_{Lb} \quad (7)$$
$$i^*_{cc} = i^*_{sc} - i_{Lc}$$

Figure 4 shows the principal scheme of the control strategy adapted to three-level shunt AF based on the synchronous current detection method.

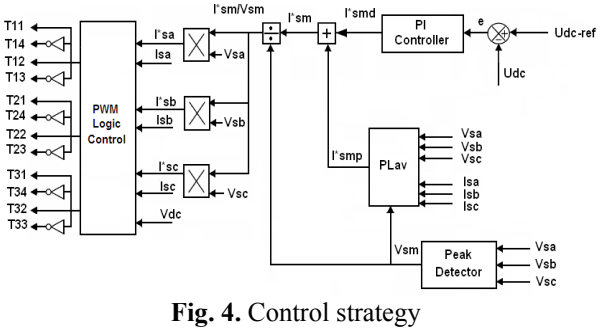

Fig. 4. Control strategy

2.2. PWM controller

To control the shunt active filter a PWM logic controller is developed. The difference between the injected current and the reference current determine the modulation wave of the reference voltage. This voltage is compared with two carrying triangular identical waves shifted one from other by a half period of chopping and generate switching pulses [21].

The control of the inverter is summarized in the two following stages:

Determination of the intermediate signals V_{i1} and V_{i2}:

- If error $E_c \geq$ carrying 1 Then $V_{i1}= 1$
- If error $E_c <$ carrying 1 Then $V_{i1}= 0$
- If error $E_c \geq$ carrying 2 Then $V_{i2}=0$
- If error $E_c <$ carrying 2 Then $V_{i2}=-1$

where V_{i1} and V_{i2} are intermediate voltage, E_c is the difference between injected and reference currents.

Determination of control signals of the switches T_{ij} and V_{i2} (i=1,2,3 ; j=1,2,3,4):

- If $(V_{i1}+V_{i2})=1$ Then $T_{i1}=1$, $T_{i2}=1$, $T_{i3}=0$, $T_{i4}=0$,
- If $(V_{i1}+V_{i2})=0$ Then $T_{i1}=0$, $T_{i2}=1$, $T_{i3}=1$, $T_{i4}=0$,
- If $(V_{i1}+V_{i2})=-1$ Then $T_{i1}=0$, $T_{i2}=0$, $T_{i3}=1$, $T_{i4}=1$.

The simulink model of the pwm logic controller is shown in Figure 3.

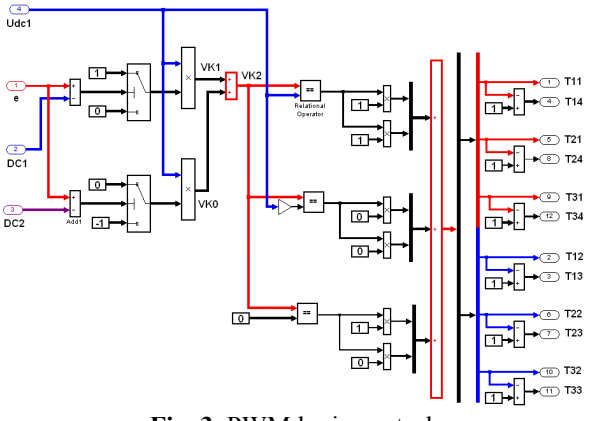

Fig. 3. PWM logic control

2.3. DC voltage controller

To maintain the dc-link voltage U_{dc} constant and compensate the inverter losses, a proportional integral controller is used to obtain the compensation current I*smd. The control loop compares the measured voltage U_{dc} with the reference voltage $U_{dc\text{-}ref}$ and generates the corresponding current I*smd given by [22]:

$$I^*_{smd} = K_p . \Delta U_{dc} + K_i \int \Delta U_{dc} . dt \quad (8)$$

where k_p and k_i are the proportional and integral gains of the PI controller and $\Delta U_{dc} = (U_{dc\text{-}ref} - U_{dc})$ is the DC bus voltage error. The overall closed-loop transfer function of the voltage controller can be expressed as:

$$\frac{U_{dc}}{U_{dc-ref}} = \frac{(K_p+(K_i/s))(K_1/(K_2 s+1))}{1+K(K_p+(K_i/s))(K_1/(K_2 s+1))}$$
$$\frac{U_{dc}}{U_{dc-ref}} = \frac{as+b}{s^2+2\zeta\omega_n s+\omega_n{}^2} \quad (9)$$

where $k_1/(K_2.s+1)$ is the transfer function of the simplified inverter, K is the voltage feedback scaling gain, ζ and ω_n are respectively the damping factor and natural angular frequency of the voltage response [23]. From (9) we can obtain $K_p = (2.\zeta.\omega_n - 1/K_1K)$ and $K_i = \omega_n^2 K_2/K_1K$.

2.4. MLPNN controllers

Artificial Neural Networks have provided an alternative modeling approach for power system applications. The MLPN is one of the most popular topologies in use today. This network consists of a set of input neurons, output neurons and one or more hidden layers of intermediate neurons. Data flows into the network through the input layer, passes through the hidden layers and finally flows out of the network through the output layer. The network thus has a simple interpretation as a form of the input-output model, with network weights as free parameters. The training cycle has two distinct paths [14]-[24], the first one is Forward propagation (it is the passing of inputs through the neural network structure to its output). The second one is the error back-propagation (it is the passing of the output error to the input in order to estimate the individual contribution of each weight in the network to the final output error). The weights are then modified to reduce the output error.

To train the neural network current controller, the Quasi-Newton Levenberg-Marquardt Training algorithm is used, it is efficient, easy to implement and is not time consuming. Computations of the algorithm proceed as follows:

1) Initialize the interconnection weights and the biases of the nodes randomly,

2) Calculate the hidden layer outputs as:

$$x_j^h = f\left(\sum_{i=1}^{ni}(x_i w_{i,j}^h)+b_j^h w_{ni+1,j}^h\right) \quad (10)$$

where x_j^h is the output of the hidden node j, x_i is the i'th input, $w_{i,j}^h$ is the weight connecting input node i with hidden node j, b_j^h is the input bias to hidden node j (normally $b_j^h=1$), $w_{ni+1,j}^h$ is the weight connecting the bias to the hidden node j, ni is the number of input nodes, and f is the sigmoid function defined as:

$$f(x) = \frac{1}{1+e^{-x}} \quad (11)$$

3) Calculate the output layer outputs as:

$$x_k^o = f\left(\sum_{j=1}^{nk}(x_j^h w_{j,k}^o)+b_k^o w_{nk+1,k}^o\right) \quad (12)$$

where x_k^o is the output of the output node k, $w_{j,k}^o$ is the weight connecting the hidden node j with output node k, b_k^o is the input bias to the output node k (normally $b_k^o=1$), $w_{nk+1,k}^o$ is the weight connecting the bias to the output node k and nk is the number of hidden nodes.

4) Calculate δ_k^o of each of the output nodes as:

$$\delta_k^o = x_k^o(1-x_k^o)(x_k^T - x_k^o) \quad (13)$$

where δ_k^o, is the error (target-output) at the output of the neuron multiplied by the derivative of f(x), x_k^T is the target output (desired output) of the output node k.

5) Calculate δ_j^h each of the hidden nodes as follows:

$$\delta_j^h = x_j^h(1-x_j^h)\sum_{k=1}^{no}\delta_k^o w_{j,k}^o \quad (14)$$

where δ_j^h is the derivative of f(x) multiplied by the summation of the weights multiplied by the output delta,

6) Adapt the weights of the output layer as:

$$w_{j,k}^o(t+1) = w_{j,k}^o(t) + \eta\delta_k^o x_j^h + \alpha\Delta w_{j,k}^o(t) \quad (15)$$

where $0<\eta<1$ is the learning constant, $0<\alpha<1$ is the momentum constant and,

$$\Delta w_{j,k}^o(t) = w_{j,k}^o(t) - w_{j,k}^o(t-1) \quad (16)$$

7) Adapt the weights of the hidden layer as:

$$w_{i,j}^h(t+1) = w_{i,j}^h(t) + \eta\delta_j^h x_i + \alpha\Delta w_{i,j}^h(t) \quad (17)$$

where,

$$\Delta w_{i,j}^h(t) = w_{i,j}^h(t) - w_{i,j}^h(t-1) \quad (18)$$

8) Repeat steps 1 to 7 until the error e is less than a prescribed small value ε.

$$\varepsilon = \sum_{k=1}^{no}\left(x_k^T - x_k^o\right)^2 \quad (19)$$

To be able to produce the correct output data, the network was trained with an improved algorithm, during the learning process the error function was minimized with an increasing number of training epochs.

Figure 5 shows the first MLPNN to use in three-level shunt active filter to replace the conventional current controller. The input pattern is the error values (Ec-a, Ec-b, Ec-c) between the measured filter currents (ifa, ifb, ifc) and the compensating reference currents (ifa*, ifb*, ifc*) whereas the outputs values are the switching states T11, T14, T12, T13, T21, T24, T22, T23,T31, T34, T32, T33 [13]. The hidden layer contains 50 neurons with a sigmoid activation function, and the output layer contains six neurons with a linear activation function. The network was trained with 10000 training examples obtained by simulation with the conventional pwm control scheme using the Levenberg-Marquardt back propagation algorithm.

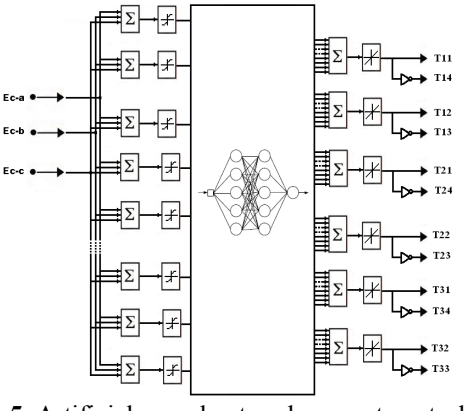

Fig.5. Artificial neural network current controller

The second MLPNN replaces the conventional proportional controller, and it is used to maintain the dc voltage across the capacitor constant and equal to Udc-ref = 800V. The input pattern is the error values ΔUdc between the measured dc voltage Udc-mes and its reference value Udc-ref. The architecture adopted for this MLPNN is a three-layer perceptron network; the hidden layer contains eight neurons with tansig activation function, whereas the output layer contains one neuron with linear activation function.

The network is trained with back propagation Levenberg-Marquardt algorithm using 30000 examples of learning (off-line) obtained by simulation-based on PI control loop. Figure 6 shows the dc voltage MLPNN controller.

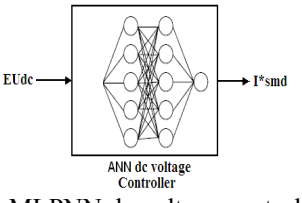

Fig. 6. MLPNN dc voltage controller

3. SIMULATION RESULTS AND DISCUSSION

The computer simulation results are provided to verify the effectiveness of the new control scheme of the three-phase three-level shunt active based on MLPNN controllers. The Matlab-Simulink simulation block diagram of the proposed SAF is shown in Figure 7. The parameters used for simulation are Lf=3mH, C1=C2=300 μF (Udc-ini=650V), Vs=220V/50Hz, Udc-ref=800V, RL=48.6Ω, LL=40 mH, PL= 5.5 kVA, fs= 10 kHz.

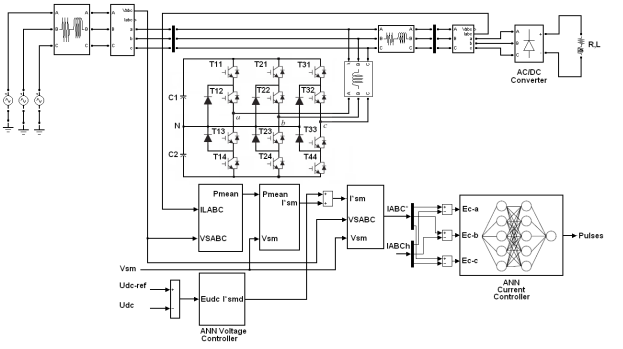

Fig. 7. Block diagram of the three-level shunt active based on MLPNNs

3.1. Three-level SAF based on conventional pwm controller

Figure 8 shows the source current waveform before compensation. The corresponding harmonic spectrum is shown in Fig. 9.

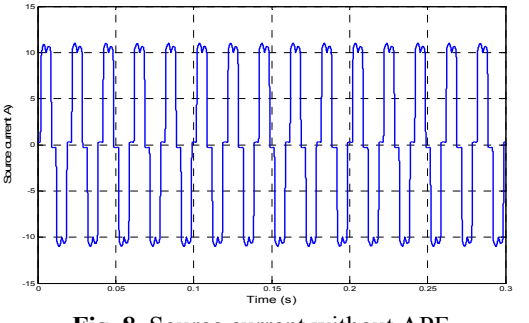

Fig. 8. Source current without APF

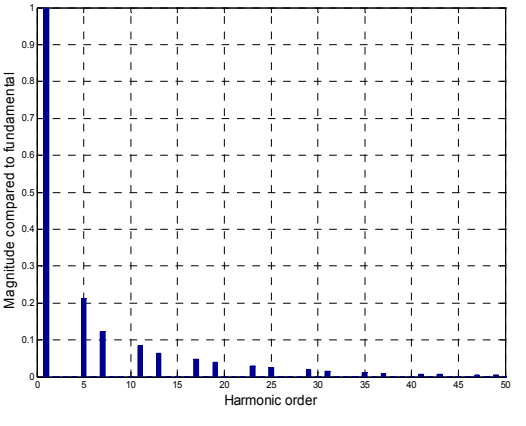

Fig. 9. Source current spectrum without APF (Fundamental (50Hz) = 11.63, THD= 27.74%)

The source and injected currents before and after APF application are shown in Fig. 10 and Fig. 11, respectively. The DC voltage is presented in Fig. 12. The waveforms of source voltage and source current are simultaneously shown in Fig. 13. The harmonic spectrum with APF is shown in Fig. 14.

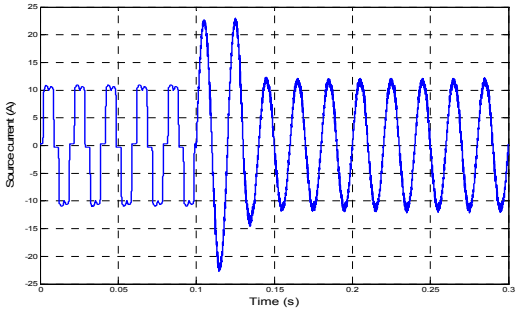

Fig. 10. Source current before and after compensation

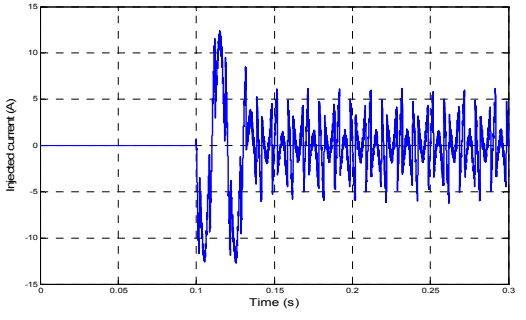

Fig. 11. Injected current

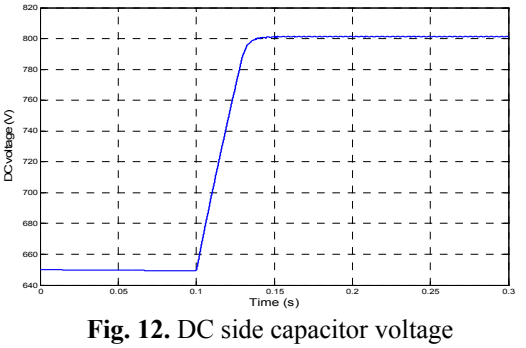

Fig. 12. DC side capacitor voltage

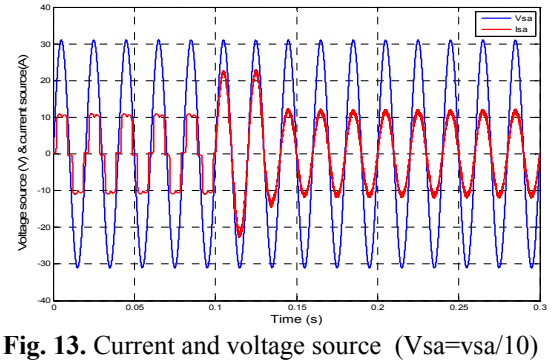

Fig. 13. Current and voltage source (Vsa=vsa/10)

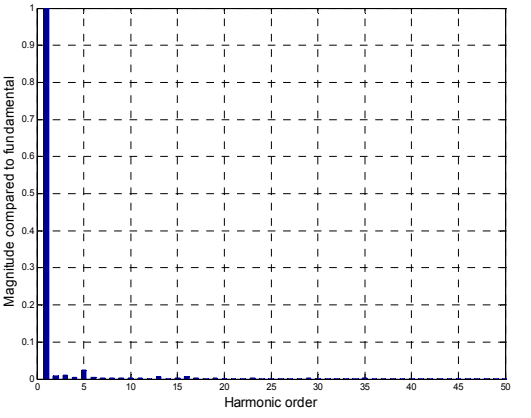

Fig. 14. Source current spectrum with APF using pwm controller
(Fundamental (50Hz) = 11.64, THD = 4.32%)

Figures 15 and 16, shows the output line voltage U_{AB}(V) and output phase voltage U_{AN}(V) when the three-level inverter is connected with the nonlinear load. The three-level voltages are approximately equal to 266V, 400V and 533Vcorresponding respectively to $U_{dc}/3$, $U_{dc}/2$ and $2U_{dc}/3$. The DC voltage reference $U_{dc\text{-}ref}$ is 800V.

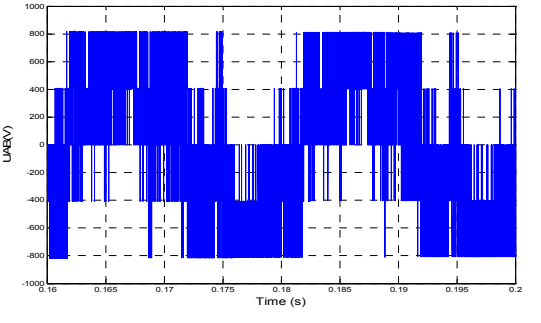

Fig. 15. Output line voltage U_{AB}(V)

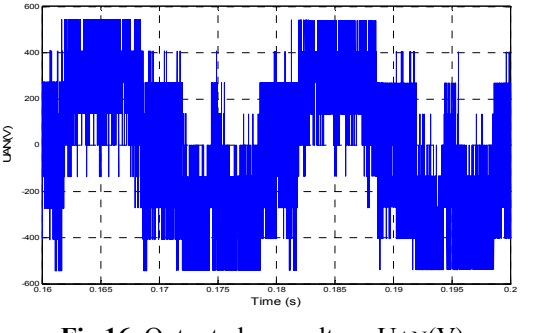

Fig.16. Output phase voltage U_{AN}(V)

3.2. Three-level SAF based on MLPNN controllers

The source current and injected current before and after APF application using MLPNN controllers are respectively shown in Figures 17 and 18. The output DC capacitor voltage is presented in Figure 19. The waveforms of source voltage with source current after

compensation are simultaneously shown in Figure 20. Finally, the harmonic spectrum of the source current after compensation is shown in Figure 21.

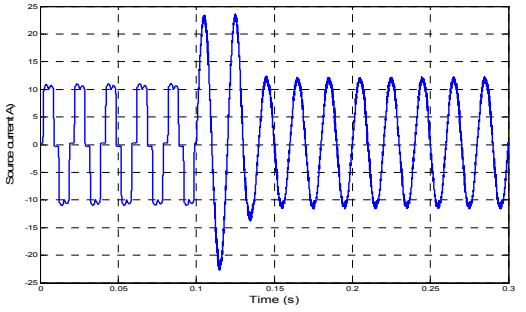

Fig. 17. Source current before and after compensation

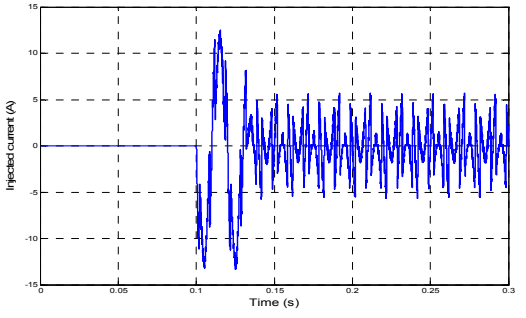

Fig. 18. Injected current

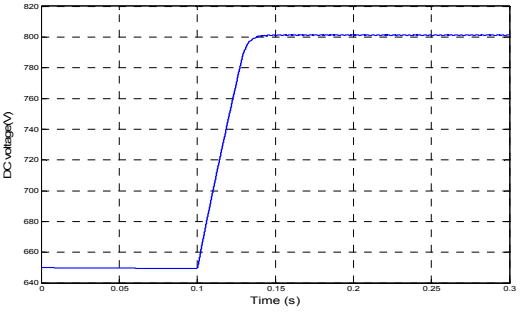

Fig. 19. DC side capacitor voltage

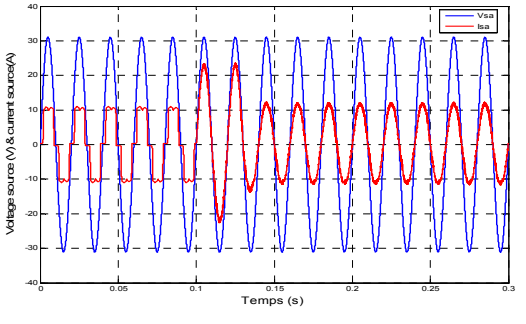

Fig. 20. Current and voltage source before and after compensation ((Vsa=vsa/10)

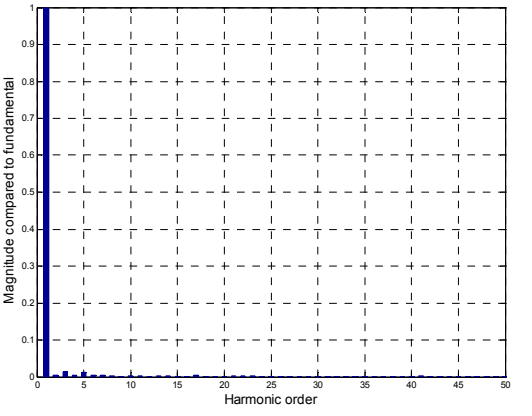

Fig. 21. Source current spectrum with APF using MLPNN controllers
(Fundamental (50Hz) = 11.65, THD= 3.96%)

3.3. Three-level SAF based on MLPNN controllers with step change in load

To study dynamic responses and test robustness of the proposed shunt active filter based on MLPNNs controllers, a step change in load (100% to 50%) is introduced between t_1 = 0.25 s and t_2 = 0.45 s. Figures 22 and 23 show the respective waveforms of source and injected current before and after compensation. The dc side capacitor voltage is presented in Fig. 24.

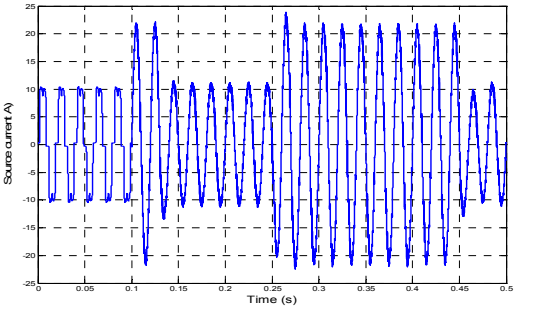

Fig. 22. Source current with step change in load

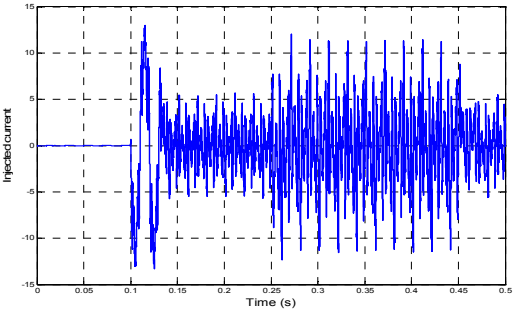

Fig. 23. Injected current with step change in load

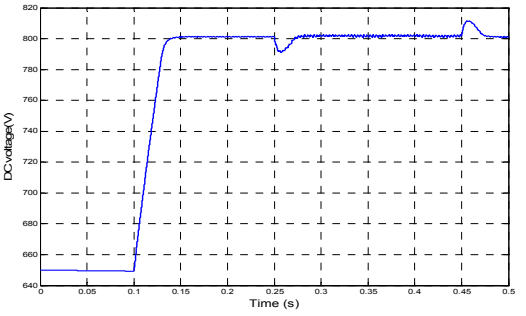

Fig. 24. DC side capacitor voltage with step change in load (between t1=0.25 s and t2=0.45s)

The current and the voltage source waveforms before and after compensation with step change in load are simultaneously presented in Fig. 25.

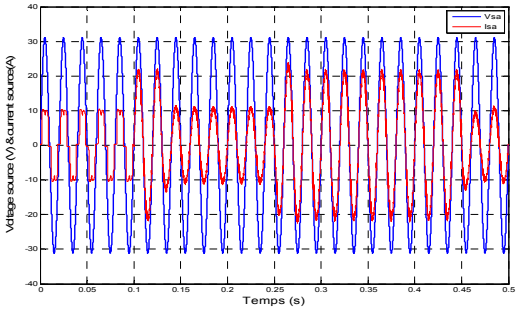

Fig. 25. Current and voltage source before and after compensation with step change in load (Vsa=vsa/10)

By visualizing Figures 10, 17 and 22, we can conclude the successful simulation of the harmonic currents compensation using the proposed control scheme. The performances of the three-level (NPC) shunt active filter based on MLPNN controllers in terms of eliminating harmonics are very acceptable. The MLPNN current controller receives the three inputs $E_{c\text{-}a}$, $E_{c\text{-}b}$, $E_{c\text{-}c}$ and generates the inverter pulses. The MLPNN dc voltage controller ensures perfectly that the voltage across the two capacitors is maintained constant and equal to $U_{dc\text{-}ref}$=800V with the fast dynamic response when a step change is introduced in load. Figures 22 and 24, illustrate the dynamic response of the proposed three-level SAF, the dc voltage pass through the transitional period of 0.03s before stabilization and reaches its reference $U_{dc\text{-}ref}$=800V with a moderate peak voltage less than 8 V (1% of $U_{dc\text{-}ref}$) when a step change in the load current is introduced between t1=0.25s and t2=0.45s. The source current pass through the same transient period of 0.03s before stabilizing, its magnitude is equal to I_{smax}= 22A (value due to the linear voltage U_{dc} between 0.1 s and 0.13s instants). This current descends approximately to 12A when the steady state is attained. Figure 25 demonstrate that the current source after active filter application is sinusoidal and in phase with the corresponding voltage source. The obtained THD values respect widely the IEEE standards Norms (THD ≤5%).

4. CONCLUSION

In this paper, a new control scheme for three-phase three-level SAF based on MLPNN controllers is presented. The developed model and simulation are performed using MATLAB-Simulink software and SimPowerSystem Toolbox. The reference currents identification uses the synchronous current detection method strategy. It's it's easy to implement and require less computation than other control methods. The first MLPNN is used to replace the conventional current controller, the second to substitute the classical proportional integral dc voltage controller. The harmonic spectrum after compensation using the proposed control scheme is widely reduced and respect IEEE standard Norms (THD<=5%). The current source after compensation is sinusoidal and in phase with the line voltage source, the power factor is nearly equal to unity. Hence, the proposed MLPNN controller is a good control system for shunt active filter based on multilevel inverter topologies for eliminating harmonics and improving the power factor with the following advantages: easy implementation, no mathematical model and few computing operations compared to the conventional hysteresis or pwm control scheme.

REFERENCES

[1] O. Vodyakho, T. Kim, S. Kwak, **"Comparaison of the space vector current controls for shunt active power filters,"** *IEEE*, pp. 612-617, 2008.

[2] U. Khruathep, S. Premrudeepreechacharn, Y. Kumsuwan, **"Implementation of shunt active power filter using source voltage and source current detection,"** *IEEE*, pp. 2364-2351, 2008.

[3] N. G. Apte, V. N. Bapat, A. N. Jog, **"A shunt active filter for reactive power compensation and harmonic mitigation,"** *The 7th International Conference on Power Electronics, IEEE*, pp. 672-676, 2008.

[4] M. Routimo, M. Salo, H. Tuusa, **"Comparaison of voltage source and current source shunt active power filter,"** *IEEE, Trans. On Power Electronics, Vol.22, Issue 2*, pp.636-643, 2007.

[5] O. Vodyakho, D. Hackstein, A. Steimel, T. Kim, **"Novel direct current-space vector control for shunt active power filters based on three-level inverters,"** *IEEE*, pp. 1868-1873, 2008.

[6] R. H. Herrera, P. Salemeron, H. Kim, **"Instantaneous Reactive Power Theory Applied to Active Power Filter Compensation: Different Approaches, Assessment, and Experimental Results,"** *IEEE, Trans. on Industrial Electronics*, pp. 184-196, 2008.

[7] S. Bhattachrya, D. Divan, **"Synchronous frame based controller implementation for a hybrid series active filter systems,"** IEEE, pp.2531-2537, 1995.

[8] Chandra A, Singh B, Al-Haddad K, **"An improved control algorithm of shunt active filter for voltage regulation, harmonic elimination, power factor correction, and balancing nonlinear loads**," *IEEE Trans. Power Electr*, pp.495-503, 2000.

[9] G. Liu, S. Su, P. Peng, **"Intelligent Control and Application of All-function Active Power Filter**," *IEEE, International Conference on Intelligent Computation Technology and Automation*, pp.1078-1081, 2008.

[10] K. Soumia, K. Fateh, **"Three-phase active power filter based on fuzzy logic controller**," *International Journal of Sciences and techniques of automatic Control & Computer engineering, Volume 3,N°1*, pp.942-955, 2009.

[11] B. R. Lin, Richard G. Hoft, **"Power electronics inverter control with neural networks**," *IEEE*, pp.128-134, 1993.

[12] B. Ren Lin, Richard G. Hoft, **"Power electronics inverter control with neural networks**," *IEEE*, pp. 900-906, 1995.

[13] A. Zouidi, F. Fnaiech, K. Al Haddad, **"Neural network controlled three-phase three-wire shunt active power filter**," *ISIE, IEEE*, (2006).

[14] M. Sarra, K. Djazia, A. Chaoui, F. Krim, **"Three-phase active power filter with integrator-proportional control**," *3rd International conference on electrical engineering*, pp. 506-511, 2009.

[15] B. Sing, K. Haddad, A. Chandra, **"A new control approach to three-phase active filter for harmonics and reactive power compensation**," *IEEE, Trans. Power Syst.13 (1)*, pp.133-138, 1998.

[16] H. Rudnick, J. Dixon, L. Moran, **"Delivering clean and pure power**, **"** *IEEE, power & Energy magazine*. pp.32-40, 2003.

[17] A. Munduate, E. Figureres, G. Garcera, **"Robust model-following control of a three-level neutral point clamped shunt active filter in the medium voltage range**," *Elsevier, Electrical Power and Energy Systems 31*, pp. 577-588, 1998.

[18] Y. Wan, J. Jiang, **"The study of FPGA-based three-level SVM NPC inverter**," *IEEE*, pp.1470-1474, 2009.

[19] E.E. El-Kholy, A. El-Hefnawy, H. M.Mahrous, **"Three-phase active power based on current controlled voltage source inverter**," *ELSEVIER, Electric power and Energy Systems 28*, pp. 537-547, 2006.

[20] S.GH Seifossadat, R. Kianinezhad, A. Ghasemi, M. Monadi, **"Quality improvement of shunt active power filter, using optimized tuned harmonic passive filters**," *International Symposium on Power Electronics, Electrical Drives, Automation and motion, SPEEDAM 2008*, pp. 1388-1393, 2008.

[21] S. Saad L. Zellouma, **"Fuzzy logic controller for three-level shunt active filter compensating harmonics and reactive power"**, *Elsevier, Electrical Power Systems Research 79*, pp.1337-1341, 2009.

[22] Y. He, J. Liu, J. Tang, Z. Wang, Yunping Zou, **"Research on control system of DC voltage for active power filters with three-level NPC inverter**," *IEEE*, pp.1173-1178, 2008.

[23] B. R. Lin, T. Y. Yang, **"Analysis and analysis of three-phase power quality compensator under the balanced and unbalanced load conditions**," *Elsevier, Electrical Power Systems Reserarch 76*, pp. 271-282, 2006.

[24] J. Y-hua, C. Yong-Wei, **"Neural network control techniques of hybrid active power filter**," *International Conference on artificial Intelligence and computational intelligence*, pp. 26-30, 2009.